INTERNATIONAL JOURNAL OF RESEARCH IN SCIENCE & TECHNOLOGY

e-ISSN:2249-0604; p-ISSN: 2454-180X

Employability Of Unsupervised Machine Learning Techniques For Elimination Of Electrodermal Activity Artefacts During And Post Surgeries

Saksham Agarwal

Montfort Sr. Sec. School, Ashok Vihar, Delhi

Paper Received: 10th February, 2021; **Paper Accepted:** 28th March, 2021;
Paper Published: 29th March, 2021

DOI: http://doi.org/10.37648/ijrst.v11i01.006

How to cite the article:

Saksham Agarwal, Employability Of Unsupervised Machine Learning Techniques For Elimination Of Electrodermal Activity Artefacts During And Post Surgeries, IJRST, January-March 2021, Vol 11, Issue1, 46-55, DOI: http://doi.org/10.37648/ijrst.v11i01.006

ABSTRACT

Detecting and removing artefacts is crucial in data preprocessing pipelines for physiological time series data, mainly when collected outside controlled experimental settings. The fact that such artefacts are often easily identifiable visually suggests that unsupervised machine learning algorithms could be practical without requiring manually labelled training datasets. Current methods are often heuristic-based, not generalizable, or designed for controlled experimental settings with fewer artefacts. In this study, we evaluate the effectiveness of three unsupervised learning algorithms—Isolation Forests, One-Class Support Vector Machine, and K-Nearest Neighbor Distance—in removing heavy cautery-related artefacts from electrodermal activity (EDA) data collected during surgeries involving six subjects. We defined 12 features for each half-second window as inputs to the unsupervised learning methods. We compared each subject's best-performing unsupervised learning method to four existing EDA artefact removal methods. The unsupervised learning method was the only approach that removed the artefacts across all six subjects. This approach can be easily extended to other types of physiological data in complex settings.

INTRODUCTION

As the collection of physiological time series data in complex, naturalistic environments become more prevalent, the data are increasingly susceptible to unexpected and uncontrollable sources of artefacts and interference. While many artefacts can be easily identified by visual inspection with minimal training, automating this process is a challenge. Existing techniques, such as thresholding signal values or derivatives, are not robust across different datasets and subjects. Supervised learning, where machine learning models distinguish between signals and artefacts using labelled datasets, has shown promise in various contexts. However, this approach is labour-intensive and impractical for artefact detection, as it necessitates manual labelling of each small-time segment across numerous training datasets.

Overcoming the challenges of artefact detection in physiological time series data is a complex task. The clear visual detectability of artifacts in most physiological time series data suggests that artifacts differ fundamentally from true signals. Our research introduces a novel and promising solution: unsupervised machine

learning methods. These methods address the time and labor constraints of traditional approaches by eliminating the need for labeled training sets and enabling the detection of complex patterns that are not explicitly defined. This innovative approach opens up new possibilities in the field of physiological data analysis, sparking curiosity and interest among researchers and data scientists.

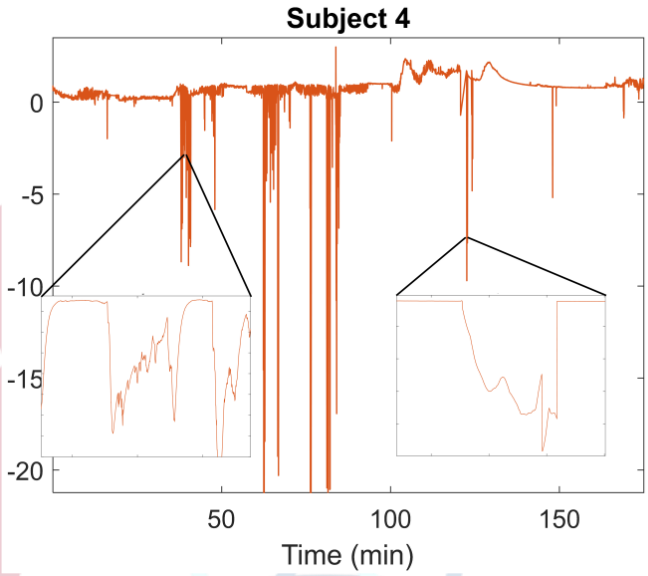

Figure 1. Raw EDA data for Subject 4 showing zoom-ins of different artifacts, where there is also true EDA data mixed in.

This paper demonstrates the effectiveness of unsupervised learning methods for detecting artefacts in electrodermal activity (EDA) datasets using just 12 well-defined features. The data were continuously collected during lower abdominal surgery in six human subjects. They were prone to motion and surgical cautery-related artefacts, which caused significant and visible deflections. Although these deflections are apparent, there are also periods of intact but shifted EDA between large deflections, and the start and end of each deflection are not marked. Additionally, deflections' magnitude, sharpness, and direction vary across subjects and datasets. This complexity underscores the depth and significance of the problem we are addressing. Figure 1 illustrates an example dataset, highlighting specific artefact characteristics.

Existing methods for artefact removal from EDA data are limited and specific to the datasets on which they were developed [4-8]. These datasets were typically collected in fully controlled or semi-controlled experimental settings, and none exhibit the same degree of artefact presence as in our study. Consequently, more than these

existing methods are needed to remove artefacts from our data altogether. We did not include supervised learning methods in our study to emphasise practicality and robustness across diverse research settings.

We evaluated three unsupervised machine learning methods for artefact detection: isolation forest [9], K-nearest neighbour (KNN) distance [10], and one-class support vector machine (SVM) [11]. We defined a set of 12 features for each half-second window to use as inputs for all the unsupervised learning methods. These features were derived from those used in existing methods, with additional features based on visible differences in the data. We also compared the performance of these unsupervised methods with existing methods. Our findings indicate that the unsupervised machine learning algorithms, utilizing the defined features, successfully removed heavy artefacts from EDA data across all six subjects, whereas the existing methods did not.

In the Methods section, we detail our datasets, the features we defined, and our implementation of the unsupervised learning algorithms. The Results section presents the EDA datasets before and after artefact removal using all methods included in the study, including existing methods. Finally, in the Discussion and Conclusion, we explain the implications of our findings and outline our plans for future work.

METHODS

A. Data

This study utilizes EDA data recorded from six subjects (two female), collected under a protocol approved by the Massachusetts General Hospital (MGH) Human Research Committee. All subjects were undergoing laparoscopic urologic or gynecologic surgery at MGH. EDA data were recorded from two digits of each subject's left hand at 256 Hz using the Thought Technology Neurofeedback System [12], starting from before the induction of anaesthesia to just after extubation. Figure 1 provides an example of raw data from one subject. The primary sources of artefacts were movements at the beginning and end of the recording, including positioning and surgical cautery. Each instance of turning the cautery on or off caused a visible deflection in the data. All data were analyzed using Matlab 2020b.

B. Features and Unsupervised Learning Methods

We defined 12 features based on guidance from the literature, listed in Table 1. These features were computed for each 0.5-second window (128 samples) for each dataset to capture the timescale of individual artefacts.

These feature vectors were then fed into three unsupervised learning methods.

- KNN Distance: This method computes the average distance between each feature vector and the nearest feature vectors in the dataset [10], using Euclidean distance and a K of 50. Artifactual data is hypothesized to have greater KNN distances than regular data.

- One-Class SVM: Similar to regular SVM, the one-class SVM is trained on data labelled as a single class representing 'normal' data and tested on data that may contain anomalies, which are assumed to be rare [11]. The one-class SVM was trained on 90% of the data, excluding the 10% with the most significant KNN distance.

- Isolation Forest: This method is similar to random forest, but each feature vector is scored based on the average path length required to isolate it as a leaf in a forest of decision trees. Artifactual data is hypothesized to have shorter path lengths than average data [9]. Each isolation forest consisted of 100 decision trees, and isolation scores were computed as the median of 10 forests.

TABLE I. FEATURES

	Feature Description
1	Standard deviation of signal
2	Difference between max and min of signal
3	Mean of first derivative
4	Median of first derivative
5	Standard deviation of first derivative
6	Min of first derivative
7	Max of first derivative
8	Mean of level 4 Haar wavelet coefficients
9	Median of level 4 Haar wavelet coefficients
10	Standard deviation of level 4 Haar wavelet coefficients
11	Min of level 4 Haar wavelet coefficients
12	Max of level 4 Haar wavelet coefficients

All three unsupervised learning methods produced scores for each data window, quantifying the bizarre nature of each segment. The isolation forest scores (IF scores) were inverted to align with the directionality of the other methods. The final step was to determine the artefact thresholds for each subject. This process leveraged the insight that data portions labelled as artefacts decrease non-continuously in discrete jumps as the threshold increases. To utilize this, the skewness and kurtosis (3rd and 4th moments) of the inter-artifact interval distribution were computed across

various thresholds. The inter-artefact interval distribution becomes more skewed as the artefact artefact proportion decreases. Thresholds corresponding to local maxima in skewness and kurtosis (indicative of significant changes in labelled artefacts) were tested. A binary search method within this set of thresholds streamlined the process, requiring the evaluation of at most five thresholds per method for each subject. The final threshold was chosen based on visual inspection to ensure artefact removal.

After identifying and removing artefacts, gaps were filled using linear interpolation to maintain continuous data. Any 'islands' of data shifted due to artifactual deflection were adjusted to match the linearly interpolated mean of the data at that time. Our method was then compared to three existing methods: variational mode decomposition, wavelet decomposition, and heuristic rule-based thresholding of data derivatives.

RESULTS

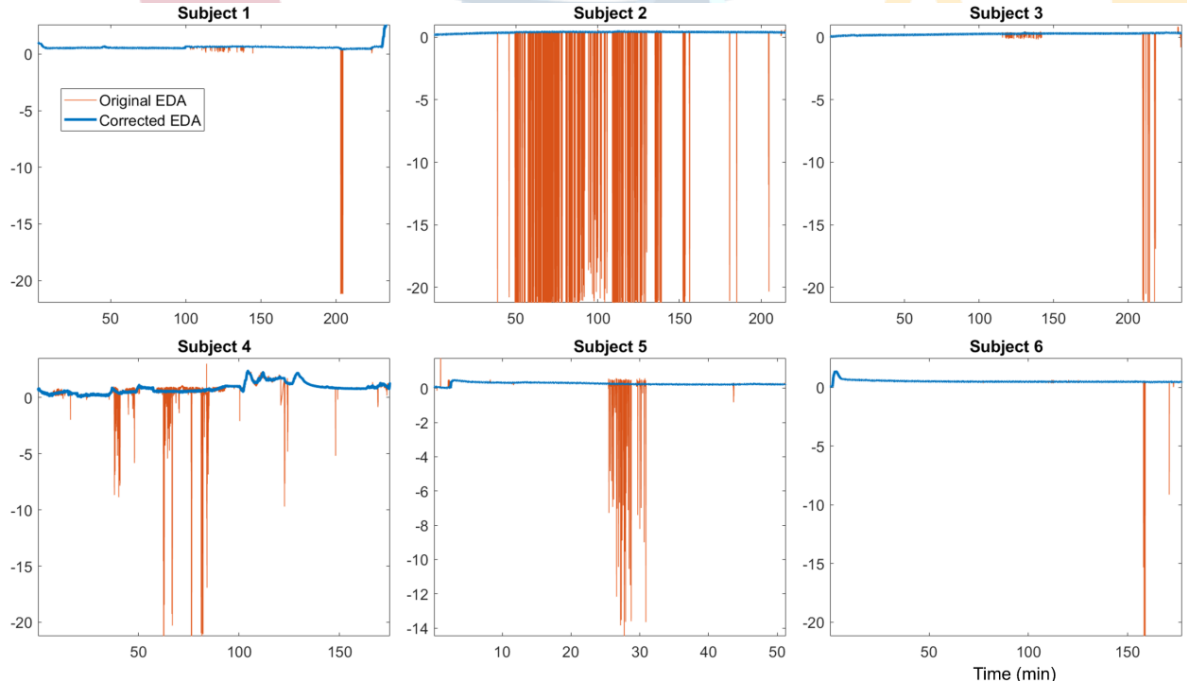

Figure 2. Uncorrected and corrected EDA for all 6 subjects.

Table II summarizes the results from all three unsupervised methods across six subjects. The artefact proportion (from 0 to 1) and the maximum contiguous artefact length are reported for each subject and method. The best method, determined by the minor proportion of artefact removed and the shortest contiguous artefact length, is highlighted in bold for each subject. Isolation forest was the best method for 3 out of 6 subjects, KNN distance and one-class SVM each for one subject, and all three methods were identical for one subject. Across all subjects, artefact proportions ranged from under 1% to just above 10%, and the longest contiguous artefacts ranged from 6 seconds to 106 seconds.

TABLE II. SUMMARY OF RESULTS

Subj	Proportion artifact Max contiguous length of artifact (sec)		
	Isolation Forest	*KNN Distance*	*1-class SVM*
1	0.0876 17.5039	0.0729 17.5039	**0.0321**[a] **17.5039**
2	**0.1030** **26.0039**	0.1169 26.5039	0.1314 26.5039
3	**0.0361** **28.5039**	0.0398 28.5039	0.0422 28.5039
4	**0.0191** **105.5659**	**0.0191** **105.5659**	**0.0191** **105.5659**
5	0.1000 14.5039	**0.0974** **14.5039**	0.1062 14.5039
6	**0.0062** **6.0039**	0.0225 6.0039	0.0149 13.5039

Figure 2 shows all six subjects' uncorrected and final corrected EDA data. Although the degree of artefact varied, we successfully removed the artefact in all cases. Figure 3 illustrates the use of kurtosis of the inter-artifact interval distribution to select the optimal threshold for Subjects 2 and 4. The local maxima of kurtosis shown in Figure 3 were tested, and the highlighted values were chosen as the final thresholds based on visual inspection of the corrected EDA data. Finally, Figure 4 compares our method with several existing methods for Subjects 2 and 4. Variational mode decomposition and wavelet decomposition were ineffective, heuristic rule-based thresholding of the EDA signal's derivative was partially effective, and only our method was fully effective in artefact removal.

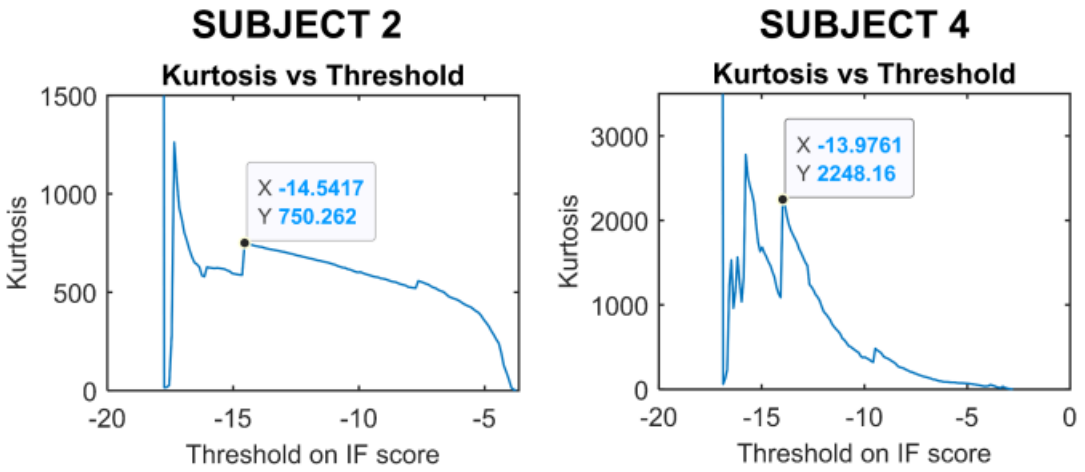

Figure 3. Use of kurtosis of inter-artifact interval distribution to select thresholds for Subjects 2 and 4. IF score refers to isolation forest score.

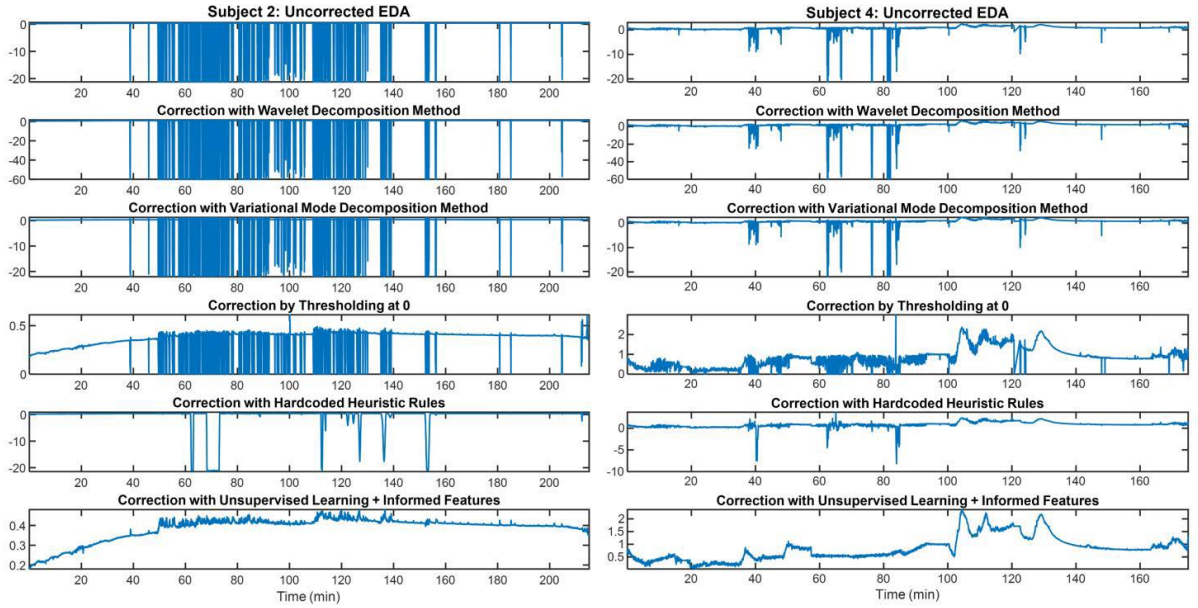

Figure 4. Comparison between different methods for Subjects 2 and 4.

CONCLUSION

In this study, we applied unsupervised machine learning methods combined with 12 features to remove heavy cautery and movement-related artefacts from six subjects' electrodermal activity (EDA) data collected during surgery. We evaluated three unsupervised learning techniques—Isolation Forest, K-Nearest Neighbors (KNN) distance, and one-class Support Vector Machine (SVM)—against existing methods such as variational mode decomposition, wavelet decomposition, and hardcoded heuristic rules. For all six subjects, the unsupervised learning methods were the

only ones that completely eliminated the artefacts. We identified the most effective unsupervised learning method for each subject by minimizing the amount of genuine EDA signal removed along with the artefact.

This approach is significant because it does not require manual labelling of a training dataset yet effectively removes heavy artefacts. Additionally, our method preserves as much of the accurate EDA signal as possible, even when interspersed with artifact-laden sections. In visibly intense artefacts, the actual proportion of data detected as artefacts was around 10% or less. In contrast, thresholding-based methods would likely remove a significant portion of the data, including accurate EDA signals. Most existing methods employ decomposition algorithms that can affect the entire signal, including regions with no artefacts. Our process, on the other hand, leaves non-artifact areas of the raw data unchanged. Most artefacts were removed in concise segments, with the longest continuous artefact lasting under 30 seconds for five out of six subjects and under 20 seconds for three.

EDA analysis typically focuses on two components operating at different timescales: tonic and phasic. The tonic component drifts slowly over tens of seconds to minutes, which can be easily interpolated when artefact sections are short. Short data durations (less than 30 seconds) for phasic EDA will likely contain a maximum of a few pulses. Moreover, dynamic methods can compute the mean and standard deviation of pulse rates over time, even if a few pulses are missing in short segments, and account for this missing data in their uncertainty estimates.

Our method utilized only 12 features for each window, many overlapping with existing methods. However, our approach allowed the AI to "learn" the differences between artefact and signal for each dataset. The physiological characteristics informed these 12 features of EDA data. This method can be expanded to similar classes of "easily visible" artefacts in other physiological data modalities, such as ECG and EEG. The physiological knowledge and types of artefacts present in those data can guide custom feature definitions.

Funding: This research has no external funding.

Conflicts of Interest: Author declares no conflict of interest.

REFERENCES

[1] G. Biagetti, P. Crippa, L. Falaschetti, G. Tanoni, C. Turchetti, “A comparative study of machine learning algorithms for physiological signal classification,” Procedia Computer Science, vol. 126, pp. 1977- 1984, 2018.

[2] M. Goldstein, S. Uchida, "A Comparative Evaluation of Unsupervised Anomaly Detection Algorithms for Multivariate Data," PLoS ONE, vol. 11, no. 4, pp. e0152173, Apr 2016.

[3] W. Boucsein, Electrodermal Activity. New York, NY: Springer, 2012.

[4] C. Qi, R.T. Faghih, "Detection of Autonomic Sympathetic Arousal from Electrodermal Activity," PowerPoint presentation (unpublished).

[5] K. Dragomiretskiy, D. Zosso, "Variational Mode Decomposition," IEEE Trans. Sig. Proc., vol. 62, no. 3, pp. 531-544, Feb. 2014.

[6] W. Chen, N. Jacques, S. Taylor, A. Sano, S. Fedor, R. W. Picard, "Wavelet-Based Motion Artifact Removal for Electrodermal Activity," in Conf. Proc. IEEE Eng. Med. Biol. Soc., pp. 6223-6226, Aug 2015.

[7] S. Taylor, N. Jacques, W. Chen, S. Fedor, A. Sano, R. Picard, "Automatic Identification of Artifacts in Electrodermal Activity Data," in Conf. Proc. IEEE Eng. Med. Biol. Soc., pp. 1934-1937, Aug 2015.

[8] Y. Zhang, "Unsupervised Motion Artifact Detection in Wrist-Measured Electrodermal Activity Data," M.S. thesis, Dept. Electric. Eng., Univ. of Toledo, Toledo, Ohio, 2017.

[9] F. T. Liu, K. M. Ting, Z-H. Zhou, "Isolation Forest," in Proc. 8th IEEE Int. Conf. Data Mining, pp. 413-422, 2008.

[10] L-Y. Hu, M-W. Huang, S-W. Ke, C-F. Tsai, "The distance function effect on k-nearest neighbor classification for medical datasets," SpringerPlus, vol. 5, no. 1304, Aug 2016.

[11] L. M. Manevitz, M. Yousef, "One-Class SVMs for Document Classification," Journal of Machine Learning Research, vol. 2, pp. 139- 154, 2001.

[12] "Neurofeedback Expert System", Thought Technology Ltd, https://thoughttechnology.com/neurofeedback-expert-system/, accessed 1/6/21.

[13] R. Barbieri, E. C. Matten, A. A. Alabi, E. N. Brown, "A point-process model of human heartbeat intervals: new definitions of heart rate and heart rate variability," Am. J. Physiol. Heart Circ. Physiol., vol. 288, no. 1, pp. H424–435, Jan 2005.